Title of the CMSC Technical Paper: Coordinate Metrology and the Proposed E57.02 Static Pose Determination Standard

Authors Names/Companies: David K. MacKinnon/ National Research Council Canada, J. Angelo Beraldin/National Research Council Canada, Tsai Hong/National Institute of Standards and Technology, Jeremy Marvel/National Institute of Standards and Technology

Contact information for submitting Author: David MacKinnon, Ph.D., P.Eng.
Measurement Science and Standards Portfolio, Emerging Technologies Division, National Research Council of Canada
1200 Montréal Road, Ottawa, ON, K1A 0R6, Canada
Phone Number: (613)993-0114

Email: david.mackinnon@nrc-cnrc.gc.ca

Word Count: 3646

Number of Images Submitted: 6

Coordinate Metrology and the Proposed E57.02 Static Pose Determination Standard

David MacKinnon[1] and J.-Angelo Beraldin
National Research Council of Canada, Measurement Science and Standards
Ottawa, Ontario, Canada, K1A 0R6

and

Tsai Hong and Jeremy Marvel
National Institute of Standards and Technology, Engineering Laboratory
Gaithersburg, Maryland, USA, 20899-1070

Abstract

We present the Proposed ASTM E57.02 "Test Method for Evaluating the Performance of Systems that Measure Static, Six Degrees of Freedom (6DOF), Pose" (Work Item ASTM WK31638) and explain why it should be considered important by coordinate metrologists. The stated purpose of the standard is to provide metrics and procedures to evaluate how well a non-contact 3D imaging system is able to determine an object's pose relative to the 3D imaging system. Pose estimation is particularly important for 3D imaging systems that can be moved during the process of generating a digital surface model of a surface, such as arm-mounted 3D imaging systems. The quality of the digital surface model generated by merging multiple depth maps depends on how well the 3D imaging system, or systems, was able to determine their pose during acquisition. We provide a summary of the document to date, the proposed test methods, and the current status of the proposed standard.

Keywords: pose estimation, ASTM, E57, non-contact 3D imaging system, standard, pose measurement system

1 Introduction

The ASTM committee E57, responsible for developing standards related to 3D imaging systems, currently has two working groups developing test methods related to non-contact 3D imaging systems. Working group WK12373[2] has been developing a method for evaluating the range error of medium-range (2 m to 150 m working distance) non-contact 3D imaging systems, while working group WK31638[3] has been developing a method for evaluating how well a non-contact 3D imaging system is able to quantify the pose of the surface being imaged. The proposed standard, however, can also be applied to systems that quantify the pose of the 3D imaging system with respect to the object. For situations in which multiple static scans must be merged to generate a digital model of a surface, pose estimation can augment or replace scan registration. We focus our discussion on the latter proposed standard and how its acceptance could impact users of non-contact 3D imaging systems, referred to in this paper simply as 3D

[1] Primary author: david.mackinnon@nrc-cnrc.gc.ca
[2] http://www.astm.org/DATABASE.CART/WORKITEMS/WK12373.htm
[3] http://www.astm.org/WorkItems/WK31638.htm

imaging systems. A 3D imaging system used to generate a pose measurement is also referred to in this paper as a pose measurement system.

In this paper we begin with background information that includes the origin of the standard test method, the test protocol and analytical procedure, and how results are to be reported. At the time of this writing, the proposed standard has completed two rounds of balloting so it can be considered a mature draft. We present an example to show how the test method would be used, then draw some conclusions before briefly describing what remains to be done with regard to this test method.

2 Background

In this section we provide some of the history behind the proposed standard. We also briefly introduce the reader to test object-based evaluation of pose measurement systems. In particular, we focus on a subset of test object-based evaluation in which the shape of the test object is the feature of interest. We referred to this as shape-based evaluation.

2.1 History

In January 2011, work began on developing a test method to evaluate how well a pose measurement system is able measure the pose (position and orientation) of an object of interest to the user's application, referred to here as a test object. Pose is represented by a 4×4 homogeneous transformation matrix

$$\mathbf{P} = \begin{bmatrix} r_{1,1} & r_{1,2} & r_{1,3} & t_x \\ r_{2,1} & r_{2,2} & r_{2,3} & t_y \\ r_{3,1} & r_{3,2} & r_{3,3} & t_z \\ 0 & 0 & 0 & 1 \end{bmatrix} = \begin{bmatrix} \mathbf{R} & \mathbf{t} \\ 0 & 1 \end{bmatrix} \tag{1}$$

with respect to an origin [1]. The test method would be applied to any non-contact 3D imaging system that has been configured to provide the pose of a user-selected test object. In this test method, a user-selected test object is used to connect the results obtained from a reference system (RS) to the results obtained from the system under test (SUT). The ability of a 3D imaging system to generate accurate pose information makes it possible to maintain information about the pose of a test object without the requirement of mechanically fixing the pose of both the test object and the imaging system. Vendors of pose measurement systems may provide performance specifications but no standard test method currently exists to guide an operator in evaluating whether their system meets those specifications.

2.2 3D Imaging Systems

The ASTM defines a 3D imaging system, in general, as any non-contact measurement system that produces a 3D representation of a surface [2]. Figure 1(a) shows how different 3D imaging system technologies compare with regard to depth measurement noise. Some of the parameters associated with a 3D imaging system include its standoff distance (distance from system to inner edge of the working volume), depth-of-field (depth of working volume), and field-of-view (width of working volume), as illustrated in Figure 1(b). The proposed standard defines a pose measurement system as "…a 3D imaging system that measures the pose of an object…" [3].

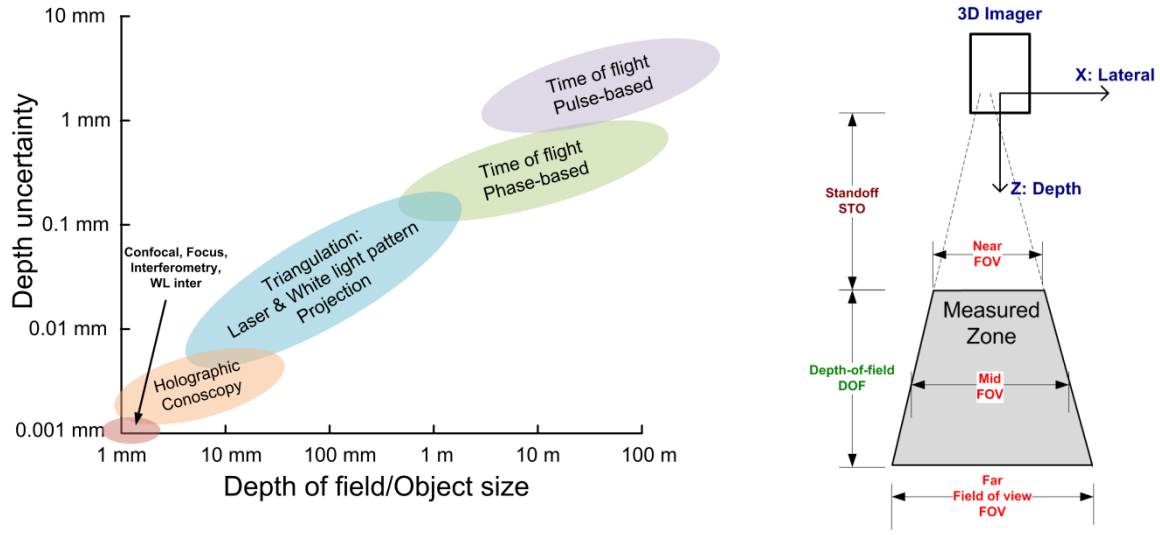

(a) (b)

Figure 1: 3D imaging systems terms. (a) Depth noise level as a function of depth-of-field for different non-contact 3D imaging methods [4]. (b) Graphical representation of terms used to describe 3D imaging systems.

3D imaging systems can also be categorized in many ways. One approach is to divide them based on their degrees-of-freedom in motion. This division is useful for assessing the complexity of the uncertainty budget associated with different systems, although uncertainty budget assessment is beyond the scope of this paper. The categories are:

- **Static 3D Imaging Systems**: 3D imaging system with fixed origin and that uses no relative movement between the imaging system and the surface being imaged to perform digitization of a single 3D image. This category includes most medium range (2 m to 150 m working distance) and some short-range (10 mm to 1 m depth-of-field) 3D imaging systems.
- **Single-Axis 3D Imaging Systems**: 3D imaging system that uses only one degree of freedom, either single-axis translational or single-axis rotational, in the motion between the imaging system and the surface being imaged to perform digitization of a single 3D image. This category consists primarily of short-range and micro-range (below 10 mm depth-of-field) 3D imaging systems
- **Multi-Axis 3D Imaging Systems**: 3D imaging system in which any type of relative motion can be used between the imaging system and the surface being imaged to perform the digitization of a single 3D image more than one degree of freedom in motion is possible. This category consists primarily of arm-mounted 3D imaging systems and hand scanners, both typically operating as short-range 3D imaging systems.

The proposed standard only applies to 3D imaging systems in which the origin of the 3D imaging system remains static during acquisition, so it applies to most Static and Single-Axis 3D imaging systems, as well as to some Multi-Axis 3D imaging systems. Moreover, it must also be possible to obtain a reference measurement of the position of the 3D imaging system during acquisition. Finally, the standard is only concerned with the ability of the 3D imaging system to determine its pose relative to an object of interest, not with the quality of the 3D representation generated by the system. This will be important for situations in which the position of the 3D imaging system is used when registering multiple scans into a 3D representation of the object of interest.

(a) (b)

Figure 2: The tetragonal antiwedge (a) and the RPAC from [6] (b) are two test objects being considered as reference surfaces for shape-based pose estimation.

2.3 Shape-based Evaluation

The test method being developed is intended for evaluating feature-based pose measurement systems for user-selected test objects specific to a particular application. However, in a shape-based system evaluation, this process requires that the test object be selected such that it minimally affects the characteristic being evaluated. In the case of pose estimation, the selected test object is one in which the uncertainty in the pose measurement obtained from the RS is limited primarily by the uncertainty in the RS. The contribution of the test object to the reference pose uncertainty should be small enough that it can be ignored. As a result, the performance of the SUT becomes, for all intents and purposes, effectively relative only to the performance of the RS.

An example of one such test object in the shape of a tetragonal antiwedge, shown in Figure 2(a). A tetragonal antiwedge is the least symmetrical of the 7 topologically distinct convex hexahedra and the simplest example of a chiral polyhedron, meaning that it is not identical to its mirror image. Using this shape, the pose of the test object could be determined unambiguously from any viewpoint. A second test object, the reduced pose ambiguity cuboctohedron (RPAC), Figure 2(b), has recently been developed and is also being explored [5, 6]. The RPAC was identified using continuous shape constraint analysis [6, 7, 8] as the shape that minimizes pose measurement errors generated by 3D imaging systems for all possible poses [6].

3 Performing an Evaluation

In this section we explain the procedure for evaluating the performance bounds of a non-contact 3D imaging system, referred to here as the system under test, with regard to a vendor's specifications pertaining to a user's application. We begin with a brief overview of the test procedure before delving into the details of the test procedure. We then conclude with how results would be reported.

3.1 Test Method

The test consists of using the SUT to place the user-selected test object in one of $N = 32$ randomly-allocated test poses within the work volume. Ideally these test poses should be evenly distributed within the area of interest, but an even distribution of test poses may not be possible for all pose estimation

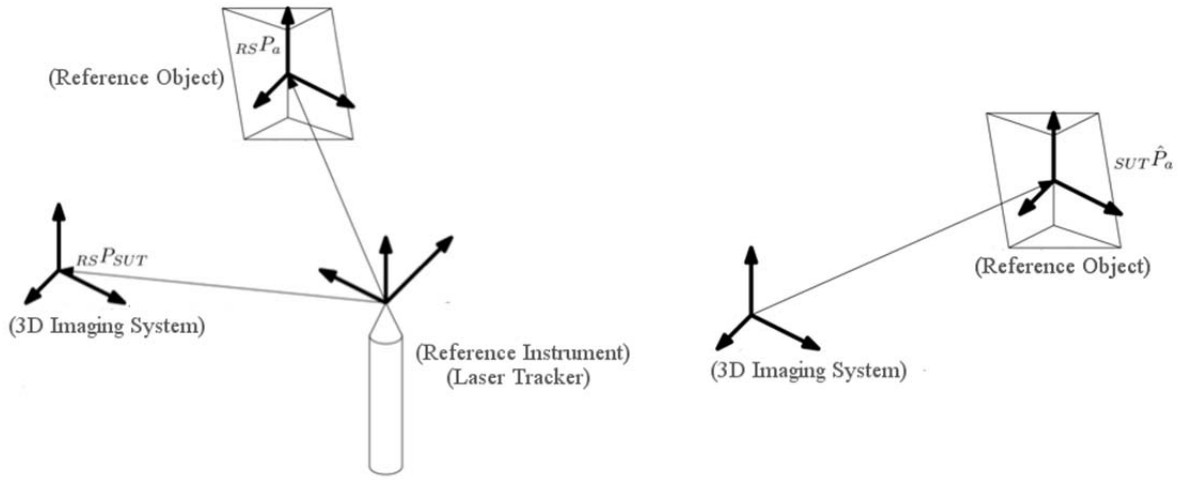

(a) (b)

Figure 3: An example of a typical test setup, in this case using a laser tracker as the RS. (a) The RS measures the pose of the SUT ${}_{RS}\mathbf{P}_{SUT}$ and the pose of the test object ${}_{RS}\mathbf{P}_a$. (b) The SUT measures the pose of the test object ${}_{SUT}\hat{\mathbf{P}}_a$ relative to the SUT.

systems. For each test pose, the SUT measures the pose of the test object ${}_{SUT}\hat{\mathbf{P}}_a$, as illustrated in Figure 3(b). In this nomenclature, the preceding subscript indicates what the pose is relative to (in this case the origin of the SUT reference frame) and the trailing subscript indicates the final pose (in this case the pose of test object). At each of the N poses, a RS is used to measure ${}_{RS}\mathbf{P}_{SUT}$ and ${}_{RS}\mathbf{P}_a$ the poses of the SUT and test object respectively relative to the RS. Figure 3(a) shows one possible test configuration in which a laser tracker is used as a RS. Once the measured and reference pose measurement values have been obtained, the pose error is calculated for the rotational and translational components of the pose measurement results.

Two types of pose error can be assessed: absolute pose error and relative pose error. Absolute pose error is the error between ${}_{SUT}\hat{\mathbf{P}}_a$ measured by the SUT and ${}_{SUT}\mathbf{P}_a$ measured by the RS. The RS does not measure ${}_{SUT}\mathbf{P}_a$ directly so it is calculated from

$$ {}_{SUT}\mathbf{P}_a = \left({}_{RS}\mathbf{P}_{SUT}\right)^{-1} {}_{RS}\mathbf{P}_a \tag{2}$$

Relative error is the error between the pose of a test object at two different locations. In the test method, the relative pose error is calculated for $N-1$ test poses relative to the first test pose. Given measured poses ${}_{SUT}\hat{\mathbf{P}}_{a_1}$ and ${}_{SUT}\hat{\mathbf{P}}_{a_k}$, the first and k^{th} poses of the test object, the measured relative pose is found by

$$ {}_{a_1}\hat{\mathbf{P}}_{a_k} = \left({}_{SUT}\hat{\mathbf{P}}_{a_1}\right)^{-1} {}_{SUT}\hat{\mathbf{P}}_{a_k}. \tag{3}$$

Similarly, the reference pose is found by

$$ {}_{a_1}\mathbf{P}_{a_k} = \left({}_{RS}\mathbf{P}_{a_1}\right)^{-1} {}_{RS}\mathbf{P}_{a_k}. \tag{4}$$

In this test method, the relative pose is always calculated relative to the first test pose.

To calculate the absolute or relative pose error, recall from (1) that $\mathbf{P}$ can be divided into rotation matrix $\mathbf{R}$ and translation vector $\mathbf{t}$. The rotational error e_R can be found using

$$0 \le e_R = \cos^{-1}\left(\frac{\text{trace}\left(\mathbf{R}\hat{\mathbf{R}}^T\right)-1}{2}\right) \le \pi \tag{5}$$

where $\hat{\mathbf{R}}$ is the measured rotation of the test object and $\mathbf{R}$ is the reference rotation of the test object, both relative to the SUT. Meanwhile, the translational error e_t can be found using the ℓ^2, or Euclidean, norm

$$0 \le e_t = \left|\mathbf{t}-\hat{\mathbf{t}}\right|_2 = \sqrt{(t_x-\hat{t}_x)^2+(t_y-\hat{t}_y)^2+(t_z-\hat{t}_z)^2} \tag{6}$$

where $\hat{\mathbf{t}}$ is the measured translation of the test object and $\mathbf{t}$ is the reference translation of the test object, both relative to the SUT. In the remainder of this document, we refer to either e_R or e_t simply as e.

The pose error $e_{i,j}$ is calculated as the difference between the reference pose and the measured pose for each test pose i. Once $e_{i,j}$ is known for all N test poses, the average pose error

$$\bar{e}_j = \frac{\sum_{i=1}^{N} e_{i,j}}{N} \tag{7}$$

is calculated for each repetition $j \in \{1,\cdots,M\}$ [9]. Note that the relative pose error cannot be calculated for test pose $i = 1$. The entire procedure is repeated between $M = 3$ and $M = 30$ times to ensure that the variation in $\bar{e}_j$ can be captured. The set of average pose errors $\mathrm{E} = \{\bar{e}_1,\ldots,\bar{e}_M\}$ is then used to evaluate the performance of the pose estimation system.

3.2 Pre-test Reporting

The test procedure begins by recording the details about the SUT and the test environment. For the SUT, we obtain the make and model of the SUT, the rated conditions (manufacturer-specified limits on operating conditions [10]), expected pose uncertainties, and the manufacturer-specified performance limits. The test method deals specifically with four performance limits, any of which may be provided by the manufacturer:

- The average error limit δ_{avg} is the maximum expected average pose error, and is tested using the Average Error Test.
- The Maximum Permissible Error (MPE) limit δ_{max} is the maximum average pose error, and is tested using the MPE Test.
- The precision error limit, represented by σ_0, is the maximum standard deviation of the average pose error, and is tested using the Precision Error Test.
- The quantile error limit δ_{quan} is the maximum p^{th} quantile of the average pose error, and is tested using the Quantile Error Test.

For the test environment, the following is recorded:

- Date, time, setup time (including warm-up) and test duration, data capture time, and post-capture processing time by SUT.
- SUT system settings.
- Ambient conditions like temperature, relative humidity, air pressure, presence of airborne particulate matter, illumination, presence and amount of vibration, and wind conditions.
- Test object details such as type of test object, surface reflectance and color, coefficient of thermal expansion, primary surface features, construction material, maximum dimensions, surface roughness, presence of deposited particulate matter, surface moisture conditions, and presence of coatings such as oil, paint, or temporary spray.

The SUT and environmental parameters are recorded as part of the test report.

3.3 Data Collection

The test procedure is performed to obtain a set of pose measurement errors of the test object with respect to the SUT.

3.3.1 Test Setup

The test setup phase begins with randomly selecting a set of N test locations from the working volume. The random locations may refer to the position of the SUT with respect to a fixed test object position, or to the position of the test object with respect to a fixed SUT position. The term "fixed" when applied to the SUT refers specifically to the origin of the SUT coordinate frame, so a SUT that incorporates one or more degrees of freedom into their scanning process (for example, a line scanner on a translation stage) are considered "fixed" if the origin of their coordinate frame is fixed during the scanning process.

For each of the N test locations, the following steps are performed:

1. For each test pose i, the test object, SUT, and RS are fixed in their respective positions as, for example, illustrated in Figure 3(a).
2. Sensor data from the SUT is used to obtain ${}_{SUT}\hat{\mathbf{P}}_a$.
3. Sensor data from the RS is used to obtain ${}_{RS}\mathbf{P}_{SUT}$ and ${}_{RS}\mathbf{P}_a$.
4. Absolute and relative pose errors are calculated as $e_{i,j}$ as described in Section 3.1.

3.3.2 Repeated Measurements

A set of average measurement errors $\{\bar{e}_1, \bar{e}_2, \bar{e}_3\}$ is obtained for each of $M = 3$ repetitions of the process described in Section 3.3.1, from which the mean $\bar{\varepsilon}_3$ and variance s_3^2 over the repetitions are obtained using

$$\bar{\varepsilon}_M = \frac{\sum_{i=1}^{M} \bar{e}_j}{M} \tag{8}$$

and

$$s_M^2 = \frac{\sum_{i=1}^{M} \left(\bar{e}_j - \bar{\varepsilon}_M\right)^2}{M-1} \tag{9}$$

respectively for $M = 3$ [9]. A fourth repetition ($M = 4$) is then performed and the mean $\bar{\varepsilon}_4$ and variance s_4^2 are similarly obtained from the augmented set $\{\bar{e}_1, \bar{e}_2, \bar{e}_3, \bar{e}_4\}$.

We decide whether to obtain another set of N measurements based on whether the variance has converged to a stable value or $M = 30$, whichever comes first. To do this, the F-statistic is calculated to test the hypothesis that $s_{M-1}^2 \le s_M^2$, with the alternative hypothesis that that $s_{M-1}^2 > s_M^2$ where $M = 4$ [9]. Rarely is $s_{M-1}^2 < s_M^2$, so we are effectively testing the hypothesis that $s_{M-1}^2 = s_M^2$. If $F > F_{0.05,M-2,M-1}$, where $F_{0.05,M-2,M-1}$ is the F-statistic for probability $\alpha = 0.05$, the numerator degrees-of-freedom $\nu_{num} = (M-1)-1 = M-2$, and the denominator degrees-of-freedom $\nu_{den} = M-1$ then the variances are still significantly different so another repetition is required. The process is then repeated for increasing numbers of repetitions M until either the variances are not significantly different or $M = 30$.

3.4 Data Analysis

The final set of average measurement errors $\{\bar{e}_1,\ldots,\bar{e}_M\}$ are used to test whether the SUT is operating within the performance limits provided by the manufacturer. The test statistics generated depend on the performance limits that have been provided and whether any particular performance limit applies to how the SUT will be used. The test statistics that may be generated are

- The expected average pose error $E(\bar{e}) = \sum_{j=1}^{M} \bar{e}_j \Big/ M$, used in the Average Error Test.
- The maximum average pose error $\bar{e}_{max} = \max_{j=1,\ldots,M} \{\bar{e}_j\}$, used in the MPE Test.
- The variance of the average pose error $s^2 = \sum_{j=1}^{M} (\bar{e}_j - E(\bar{e}))^2 \Big/ M-1$, used in the Precision Error Test.
- The p^{th} quantile of the average pose error q_p, used in the Quantile Error Test.

We briefly describe how each of the associated tests is performed.

3.4.1 Average Error Test

Given δ_{avg} provided by the manufacturer and $E(\bar{e})$ obtained from the SUT relative to the RS, if

$$\frac{E(\bar{e}) - \delta_{avg}}{\sqrt{s^2/M}} > t_{\alpha,M-1} \tag{10}$$

then the SUT is operating outside the performance limit provided by the manufacturer. The test statistic $t_{\alpha,\nu}$ is cumulative distribution of the probability density function (PDF) of the t-distribution [9] with probability $\alpha = 0.05$ and degrees-of-freedom $\nu = M-1$.

3.4.2 MPE Test

Given δ_{max} provided by the manufacturer and $\bar{e}_{max}$ obtained from the SUT relative to the RS, if

$$\frac{\delta_{max} - \bar{e}_L}{\bar{e}_L - \bar{e}_S} > \frac{1-\alpha}{\alpha} \tag{11}$$

then the SUT is operating outside the performance limit provided by the manufacturer. The variables $\bar{e}_L$ and $\bar{e}_S$ are the largest and second-largest elements of $\{\bar{e}_1,\ldots,\bar{e}_M\}$ respectively. This is referred to as the Robson-Whitlock Test, which is described in [11] and [12].

3.4.3 Precision Error Test

Given σ_0 provided by the manufacturer and s^2 obtained from the SUT relative to the RS, if

$$\frac{(M-1)s^2}{\sigma_0^1} > \chi^2_{\alpha,M-1} \tag{12}$$

then the SUT is operating outside the performance limit provided by the manufacturer. The test statistic $\chi^2_{\alpha,\nu}$ is the cumulative distribution of the Chi-squared PDF [9] with probability $\alpha = 0.05$ and degrees-of-freedom $\nu = M - 1$.

3.4.4 Quantile Error Test

Given δ_{quan} provided by the manufacturer and q_p obtained from the SUT relative to the RS, if $\aleph < b_{M,\alpha}$ then the SUT is operating outside the performance limit provided by the manufacturer. The test statistic $b_{M,\alpha}$ is the upper quantile of the binomial PDF [13] with probability $\alpha = 0.05$, and $\aleph$ is the number of elements of $\{\bar{e}_1,\ldots,\bar{e}_M\}$ for which $\bar{e}_j \le \delta_{quan}$ is true.

3.5 Reporting of Results

Once all tests have been completed, a test report is generated. The report identifies the laboratory in which the testing was conducted, the operator (individual or team) who conducted the test, and the contents of the pre-test report described in Section 3.2. The report then presents a summary of the performance limits tested and the test result. An appendix is attached to the report consisting of all pose measurement results (both SUT and RS) from all test poses and repetitions, the within-test pose average pose errors, and the number of repetitions.

4 Conclusions

A Proposed Standard ASTM E57.02 "Standard Test Method for Evaluating the Performance of Systems that Measure Static, Six Degrees of Freedom (6DOF), Pose" is currently under development by the ASTM. The purpose of the test method is to provide metrics and procedures to evaluate how well a non-contact 3D imaging system is able to determine an object's pose. For some systems, the quality of the surface model generated by merging multiple depth maps depends on how well the 3D imaging system, or systems, was able to determine their pose during acquisition. As a result, this test method should be of interest to metrologists who work with 3D imaging systems that pre-register multiple depth maps, or those that also provide pose information to assist in registration during post-processing. We presented a summary of the document to date, the proposed test methods, and the current status of the proposed standard.

5 Acknowledgments

We extend our thanks to the ASTM work group whose hard work made the proposed standard a possibility. In particular, we acknowledge the written contributions of Mili Shah, Charles Hagwood, Chad English, and Gerry Cheok.

References

[1] Niku, Saeed B., *Introduction to Robotics: Analysis, Systems, and Applications*, Prentice Hall, Upper Saddle River, NJ, 2001.

[2] ASTM E2544-11a: *Standard Terminology for Three-Dimensional (3D) Imaging Systems*, The American Society for Testing and Materials (ASTM International), 2011.

[3] ASTM WK31638: *Standard Test Method for Evaluating the Performance of Systems that Measure Static, Six Degrees of Freedom (6DOF), Pose*, The American Society for Testing and Materials (ASTM International), 2013.

[4] Robson, S., Beraldin, A., Brownhill, A., MacDonald, L., *Artefacts for optical surface measurement*, Society of Photo-Optical Instrumentation & Electronics & Society for Imaging Science and Technology, in Videometrics, Range Imaging, and Applications XI (2011).

[5] Mark, L. H., Okouneva, G., Saint-Cyr, P., Ignakov, D., and English, C., "Near-optimal Selection of Views and Surface Regions for ICP Pose Estimation," in *Advances in Visual Computing: Proceedings of the 6th International Symposium*, Vol. 6454(Part II): pp. 53–63 (2010), Springer-Verlag.

[6] English, C., Okouneva, G., Saint-Cyr, P., Choudhuri, A., Luu, T., "Real-Time Dynamic Pose Estimation Systems in Space: Lessons Learned for System Design and Performance Evaluation," in *International Journal of Intelligent Control and Systems*, Vol. 16(2): pp. 79-96 (2011).

[7] Okouneva, G., McTavish, D., and Okunev, O., "Selection of Regions on a 3D Surface for Efficient LIDAR-based Pose Estimation," in *Proceedings of the Vision, Modeling, and Visualization Workshop*, pp. 387-388 (2009).

[8] McTavish, D. J. and Okouneva, G., "A New Approach to Geometrical Feature Assessment for ICP-Based Pose Measurement: Continuum Shape Constraint Analysis," in *Proceedings of the International Machine Vision and Image Processing Conference*, pp. 23–32 (2007).

[9] Mendenhall, W., Scheaffer, R.L., and Wackerly, D.D., *Mathematical Statistics with Applications*, Duxbury Press, Boston, MA (1981).

[10] ASME B89.4.19-2006: *Performance Evaluation of Laser-Based Spherical Coordinate Measurement Systems*, The American Society of Mechanical Engineers (ASME), 2006.

[11] Robson, D.S. and Whitlock, J.H., "Estimation of a Truncation Point," in *Biometrika*, Vol. 51(1 and 2): pp. 33-39 (1964).

[12] Cooke, P., "Statistical inference for bounds of random variables," in *Biometrika*, Vol. 66(2): pp. 367-374 (1979).

[13] Conover, W.J., *Practical Nonparametric Statistics*, 2nd edition, Wiley, NY (1980).